Journal of Engineering Physics and Thermophysics, Vol. 79, No. 6, 2006

THERMAL PERFORMANCE ANALYSIS OF SILICA TILES

K. N. Shukla,[a] A. Pradeep,[b] and S. S. Suneesh[2]

UDC 629.7.018.3:536.24+536.33

The thermal response of nonablating ceramic tiles is studied by the finite-element method. A continuum model is used to determine the thermal conductivity of porous materials. The temperature distribution for the one-dimensional model is compared with the available arc-jet result. Also presented are the 2D and 3D temperature contours and the heat-flux distributions for silica tiles. The expression for the pressure distribution in a silica tile is derived.

Introduction. The design of a thermal protection system (TPS) for higher temperature applications involves the modeling and synthesis of various nonlinear coupled systems. The design of a TPS, which is an interface between the entry flow environment and the spacecraft, is based on the aerothermodynamic predictions of quantities such as the surface temperature, heat-transfer rate, shear, and pressure loads. Ablating and nonablating materials are the two important classes of TPS used for design of the entry vehicle. A nonablating TPS is generally used on reusable vehicles. The energy conducted into the vehicle is mimimized due to minimization of radiation from the body and low thermal conductivity of the TPS. For the materials mentioned, the flow environment is altered by chemical reaction that occurs on the surface of the TPS. This surface catalysis reaction increases surface heating and alters temperature gradients within the boundary layer [1–4]. The silica tile with a black glazed surface is one of the candidate materials for a nonablating TPS. The low catalytic efficiency of the reaction minimizes the surface heating.

Rigid tiles are made from high-purity silica fibers, which are rigidly interconnected in a high-temperature sintering process. Tiles with densities of 144 and 352 kg/m^3 have been realized. The exposed tile surface is covered with a thin glassy coating, which is black for the hottest areas of the space vehicles and white elsewhere. The tiles are bonded to a felt pad, which, in turn, is bonded to the vehicle skin. In both bonds, a room-temperature vulcanized (RTV) material is used. The designed gaps between the tiles make the system flexible and allow gases to vent when required. Depending on the size of the gap, it either is kept empty or filled by a gap filler. In reentry, the flow of gases around the vehicle changes from laminar to turbulent. The later this change, the less the total heat load. It is therefore important that the surface of the vehicle be relatively smooth to prevent local turbulence. To minimize the heat load, the gas fillers must be fitted perfectly in the intersections and the gaps between the tiles. The gap must be carefully exhausted and smoothened in order to prevent surface irregularities.

In the present investigation, the temperature distribution of the TPS tiles is calculated by coupling the thermal response and thermal conductivity programs. The thermal conductivity of the tile is determined using the model described and the temperature distribution is predicted by a finite-element computer program with the software package MSC NASTRAN/PATRAN. An expression is derived for the internal pressure in the silica tiles.

Thermal Conductivity. The tiles consist of porous material. The structure shape of the solid matrix varies within wide limits. It may, for instance, be composed of cells, fibers, or graves. In general, a uniform distribution of void sizes is nonexistent. Because of the complexities of the mechanism involved in the diffusion processes through the irregular void configuration in porous bodies, the subject is not yet completely developed. We attempt here to derive an expression for the thermal conductivity of the tiles, assuming that they are continuous.

We consider a porous body with the bound matter filling the voids in an unsaturated state. This matter consists of liquid, vapor, and inert gas at a temperature above 273 K and of ice, supercooled liquid, and gas at a temperature below 273 K. There are vapor and air in the pores and capillaries of the porous body [5]. Since we are

[a]Karunya University, Coimbatore-641114, India; email: kn_shukla@rediffmail.com; [b]College of Engineering, Thiruvananthapuram-695016, India. Published in Inzhenerno-Fizicheskii Zhurnal, Vol. 79, No. 6, pp. 107–113, November–December, 2006. Original article submitted November 16, 2005; revision submitted January 3, 2006.

1062-0125/06/7906-1157

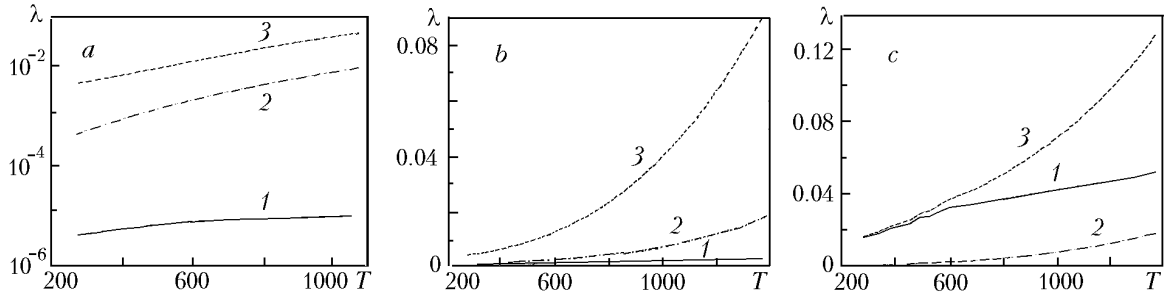

Fig. 1. Thermal conductivity of TPS tile as a function of temperature at pressure P = 0.0001 (a), 0.01 (b), and 1 atm (c): 1) gas; 2) radiative; 3) total. T, K; λ, W/(m·K).

interested in high-temperature application, it is reasonable to assume that the pores are filled with air/inert gas. The heat transfer can be attributed to heat conduction in both solids and gas and to radiation.

Thermal conductivity of gas. The thermal conductivity of a gas can be expressed as

$$\lambda_g = \frac{\lambda_a}{1 + 2\beta \mathrm{Kn}} . \tag{1}$$

Here, λ_a is the thermal conductivity of a gas at atmospheric pressure and Kn is the Knudsen number, defined as the ratio of the mean free path l_g of the gas enclosed in the pores to the pore diameter δ (Kn = l_g/δ). The value of l_g is determined by the following expression given by Sutherland [6]:

$$l_g = \frac{C_1 (P_g)}{1 + C_2/T} ,$$

where the constants C_1 and C_2 for different gases have been tabulated by Ardenne [7]. The correcting factor β is a function of the ratio of the specific heats of the gas at constant pressure and constant volume and can be taken as 1.63.

The radiative thermal conductivity is calculated using the diffusion model described by Howell and Siegel [8]:

$$\lambda_r = \frac{16\sigma n^2}{3E} T_r^3 , \tag{2}$$

where E is the extinction coefficient and

$$T_r^3 = \frac{(T^2 + T_a^2)(T + T_a)}{4} . \tag{3}$$

We can thus determine the total thermal conductivity of the bulk material as a linear combination of the conductivities of the solid, gas, and radiation as suggested by Stewart and Leiser [10]:

$$\lambda_t = \eta f_1 (V_s) \lambda_s + (1 - V_s) \lambda_g + \tau f_2 (V_s) \lambda_r , \tag{4}$$

where $f_1(V_s) = V_s$ and $f_2(V_s) = 1/V_s$ are the weighting factors.

Linear dependences for parameters η and τ result in the following expressions [9]:

$$\eta = 1.93 V_s ,$$

$$\tau = -8.571 (1 - V_s) + 0.84 \quad \text{for porosity} > 0.84 ,$$
$$\tau = 1.2 \quad \text{for porosity} < 0.84 .$$

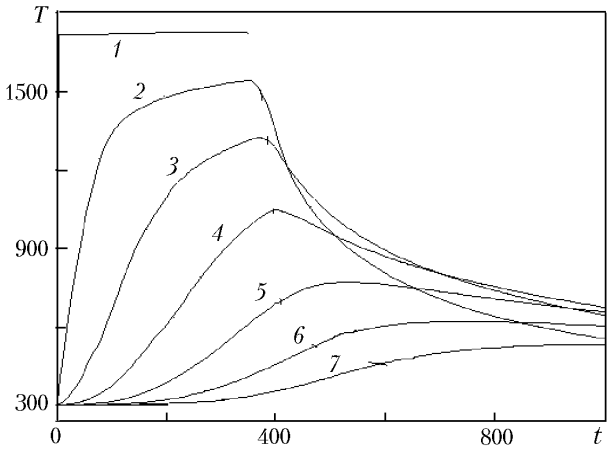

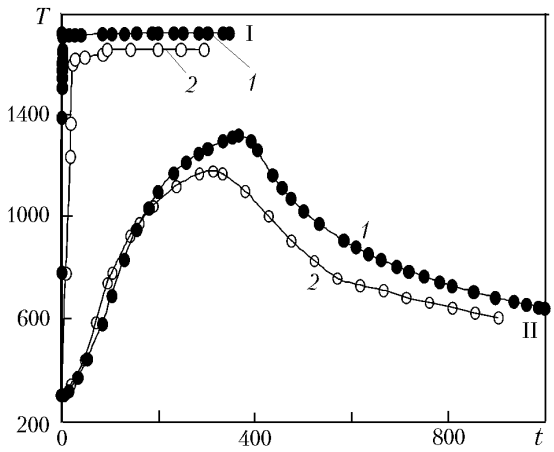

Fig. 2. Transient temperature in a silica tile for the first seven nodes with 1D analysis. *t*, sec; *T*, K.

Fig. 3. Comparison of calculated temperature (1) with measurement results (2) at the first (I) and second (II) nodes. *t*, sec; *T*, K.

The two adjusted parameters η and τ, which relate to solid conduction and radiation heat transfer, were found to be independent of fiber composition and structure and to depend only on the solid volume fraction (on the porosity).

Effective thermal conductivity values for silica insulations at different pressures are shown in Fig. 1a, b, and c. The thermal conductivity of a solid [0.005 W/(m·K)], which is not shown in the figures, is taken into account when the total thermal conductivity is calculated. The computations show that the overall effective thermal conductivity profile is substantially influenced by the radiation thermal conductivity λ_r at a high temperature. Equation (4) predicts values of the conductivity for $P < 1$ atm that are similar to those determined by the Ames Engineering Model [10]. For $P > 1$ atm, this expression gives higher values

Heat-Transfer Analysis. The primary objective of the study is to predict the thermal response of the reusable surface insulations (RSI). Aerothermal heat flux is applied on the surface of the RSI for a fixed time and then it is withdrawn. Heat is reradiated from the surface to deep space as well as conducted through the TPS component. The RSI and the TPS tube are porous ceramic materials. Their emittance [8] and specific heat are functions of temperature and pressure. If required, the thermal properties of the model are extrapolated as linear.

The governing equation for heat transfer in a solid is written as

$$\rho c_p \frac{\partial T}{\partial t} = \nabla (\lambda \nabla T) \tag{5}$$

and satisfies the boundary and initial conditions

$$T(x, 0) = T_0 , \tag{6}$$

$$\lambda \left(\frac{\partial T}{\partial x} \right)_{x=a} = q - \varepsilon \sigma T^4 , \tag{7}$$

$$\lambda \left(\frac{\partial T}{\partial x} \right)_{x=b} = 0 . \tag{8}$$

For design purposes, generally a 1D thermal analysis is sufficient to determine the transient temperature response near the center of the tiles for stagnation heating. Aero-thermal heat flux can be expressed in the form of a

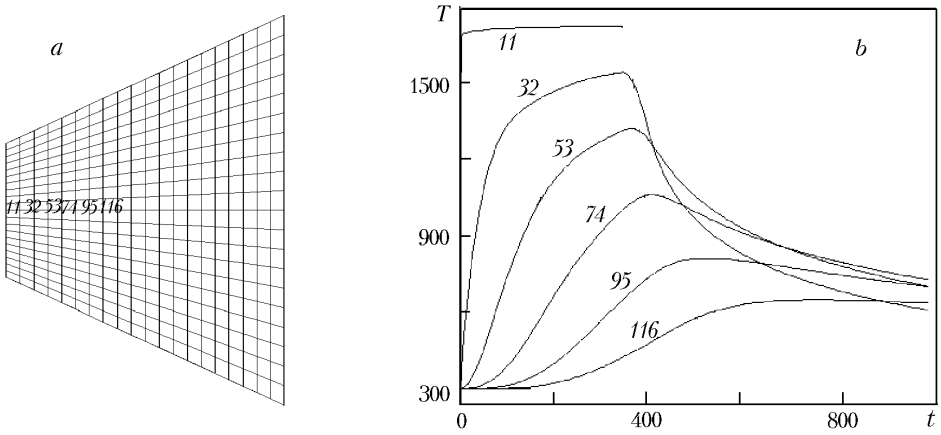

Fig. 4. 2D rectangular elements of a silica tile (a) and transient temperature for the corresponding nodes (b). t, sec; T, K.

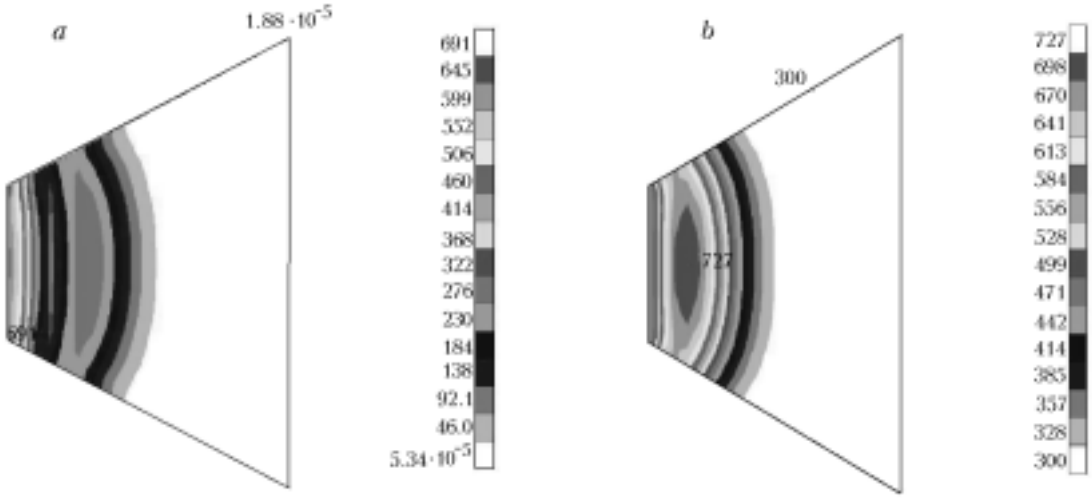

Fig. 5. Heat flux (a) and temperature (b) distributions on a silica tile. q, kW/m^2; T, K.

unit step function [$q(t) = qU(t—t_0)$], where the heat flux is withdrawn from the moment t_0. The accuracy in evaluation of the thermal conductivity plays a major role in determining the accuracy of the calculated temperature response.

The tile is divided into 20 nodes of equal size. Figure 2 shows the temperature response in depth for the first seven nodes of the TPS tiles when a heat flux of 400 kW/m^2 is applied at one end. The numbers in the figure correspond to the node numbers. The rod absorbs a part of the heat flux and the remainder is reflected. The rod takes a temperature of 1720 K due this high heat flux.

The following properties of the silica tile were used to predict the thermal conductivity for the insulation material through Eqs. (1)–(4): ρ = 352 kg/m^3; V_s = 0.8; δ = 0.8 μm; E = 14,900 m^{-1}. The values of the thermal conductivity at different temperatures were used in the finite-element program to determine the temperature distributions in the tiles. This analysis helps us to find the way a tile responds to a high heat load from one end to another.

Figure 3 gives a comparison of the present results with the measured values of Stewart and Leiser at nodes 1 and 2, respectively [10]. The present software results in a temperature that is about 5% higher than the measured one, which may be erroneous due to uncertainty in the measurement.

For a detailed study, a 2D finite element analysis [11] was carried out to determine the temperature response of the silica tiles. Figure 4a presents the nodal discretization of the silica tile as used for the measurement in the experiment of Stewart and Leiser [10]. Figure 4b shows the time history of the temperature in the tile in depth for the corresponding nodes on the basis of the 2D model. Within a few seconds, the tile reaches a high temperature of 1720

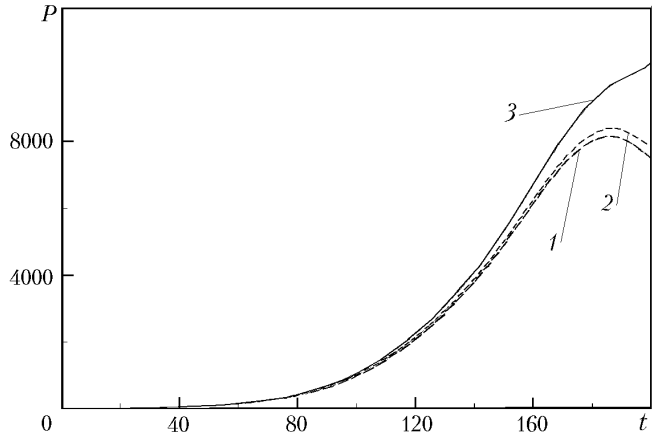

Fig. 6. Calculated transient pressure for a typical trajectory for different values of the parameter A: 1) A = 1; 2) 5; 3) 7. t, sec; P, Pa.

K. After 400 seconds, the temperature begins to decrease due to reduction in the heat load. The thermal response from the 2D analysis is very similar to that of the 1D analysis. The initial and boundary conditions for the 2D analysis are the same as given by Eqs. (6)–(8). The other two edges are assumed to be insulated.

As the conditions on the surface for the given analysis, the pressure P = 0.01 atm and heat flux q = 400 kW/m^2 were taken. Predictions were made with thermal conductivity values obtained by using Eq. (4). The measured in-depth temperature histories were compared with the earlier results of Stewart and Leiser. The results obtained give a very good agreement with these experimental values.

The heat flux applied to the material varies with time. Here, the analysis was done for a time period of 1000 sec. After 400 sec, the heat-flux value is zero. Hence, the surface temperature reaches 1720 K for 400 sec and then begins to decrease. The heat flux penetrates through the material and Fig. 5a shows the variation of its intensity along the tile material at the moment of 1000 sec. The corresponding temperature contours are shown in Fig. 5b. It is seen that the maximum temperature is 727 K, which means that the temperature decreases to the moment of 1000 sec.

Refractory Vent. The internal pressure of the gas vented through the porous tiles can be described by the Darcy law as

$$\dot{m} = -\frac{\pi D^2}{4}\frac{K\rho}{\mu}\frac{dP}{dx} \tag{9}$$

or, using the ideal gas law

$$\rho = \frac{M}{RT}P\,, \tag{10}$$

as

$$\dot{m} = -\frac{\pi D^2}{4}\frac{M}{RT}\frac{KP}{\mu}\frac{dP}{dx}\,. \tag{11}$$

Here, we have assumed constant internal temperature and negligible gas storage in the vent [12].

To account for increased mass flow due to slip, the effective porosity is expressed by the following relation:

$$K = K_0\left(1 + \frac{b}{P}\right),$$

where b is a constant. Substituting this expression into (11), we can integrate the obtained equation for the isothermality condition

$$\dot{m}L = \frac{\pi D^2}{4}\frac{M}{RT}\frac{K_0}{\mu}\left[\frac{P^2 - P_{\text{ext}}^2}{2} + b\,(P - P_{\text{ext}})\right]. \tag{12}$$

Since

$$m = V\rho = \frac{M}{RT}VP\,,$$

Eq. (12) can be rewritten as

$$\frac{dP}{dt} = \frac{AK_0}{\mu}\left[\frac{P^2 - P_{\text{ext}}^2}{2} + b\,(P - P_{\text{ext}})\right], \tag{13}$$

where

$$A = \frac{\pi D^2}{4}\frac{1}{LV}\,.$$

For the reentry environment, P_{ext} is the prescribed function of time. Equation (13) can be numerically integrated to determine the internal pressure inside the porous tiles. Figure 6 shows the predicted pressure experienced by a space recovery module with some values of A for a typical trajectory. Depending upon the maximum pressure differences allowed, the vent dimension could be easily determined.

Conclusions. The computerized thermal analysis offers a powerful tool for time and cost effective estimation of the performance of RSI or TPS tiles. Some of its applications have been demonstrated in the current study. The models used were compared, whenever possible, with the experimental arc-jet data.

The expression for thermal conductivity was derived based on the continuum theory of a porous body. The heat-conduction equations resulted in successful calculation of the temperature response in depth of silica tiles subjected to a very high heat flux. The assumptions used in the computations included an adiabatic back wall, low surface catalysis, and absence of convective cooling during soaking out.

An analytical expression for the pressure distribution inside the tile, from which one can determine the venting area for a required pressure difference, is derived.

This work is a part of the M. Techn. Thesis of A. Pradeep (carried out at the Vikram Sarabhai Space Center (VSSC), Trivandrum), who thanks Shree Shailendra Tiwari for help in the use of the MSC NASTRAN/PATRAN package and Shree Haridas for the computer facilities of VSSC.

NOTATION

c_p, specific heat at constant pressure; D, tile diameter; E, extinction coefficient; K, permeability; K_0, effective permeability; Kn, Knudsen number; L, thickness; M, molecular weight; m, mass; $\dot{m}$, mass flow rate; n, refractive index; P, pressure; q, heat flux; R, gas constant; T, temperature; V, gas volume; V_s, volume fraction of solid; x, coordinate; σ, Stefan–Boltzmann constant; β, density scale factor; δ, pore diameter; ε, emittance; η and τ, bonding factors; λ, thermal conductivity; μ, viscosity; ρ, density. Subscripts: a, atmosphere; ext, external; g, gas; r, radiation; s, solid; t, total.

REFERENCES

1. J. V. Rakich and M. J. Lanfranco, Numerical computation of space Shuttle laminar heating and surface streamlines, *J. Spacecraft Rockets*, **14**, 265–272 (1977).
2. D. A. Stewart and D. B. Leiser, Thermal response of integral, multicomponent composite thermal protection systems, in: *Proc. AIAA 20th Thermophysics Conference*, Williamsburg, VA, June 19–21, 1985, pp. 420–427.
3. S. A. Chiu and W. C. Pitts, Reusable surface insulations for reentry spacecraft, *AIAA Paper* 91-0695 (1991).
4. K. Daryabeigi, Thermal analysis and design optimization of multilayer insulation for reentry aerodynamic heating, *J. Spacecraft Rockets*, **39**, No. 4, 509–514 (2002).

5. K. N. Shukla, *Diffusion Processes during Drying of Solids*, World Scientific, Singapore (1991).
6. W. Sutherland, The viscosity of gases and molecular force, *Phil. Mag.*, **36**, 507–531 (1983).
7. M. Ardenne, *Tabellen zur Angewandten Physik*, Vol. III, VEB Deutscher Verlag der Wissenschaften, Berlin (1973).
8. J. R. Howell and R. Siegel, *Thermal Radiation Heat Transfer*, McGraw-Hill, Tokyo (1981).
9. S. A. Chiu, Thermal analysis of reusable surface insulations, *AIAA Paper* 92-0852 (1992).
10. D. A. Stewart and D. B. Leiser, Characterization of the thermal conductivity for advanced toughened unipiece fibrous insulations, *AIAA Paper* 93-2755 (1993).
11. PATRAN Plus User Manual, PDA Engineering Mesa, C. A., July (1988).
12. J. Marshall and F. S. Milos, Gas permeability of rigid fibrous refractory insulations, *AIAA Paper* 97-2479 (1997).